



Computational and Experimental Studies on the Effect Back Pressure on Twist Extrusion Process

Mehran Nouri¹ · Hamidreza Mohammadian Semnani¹ · Esmail Emadoddin¹

Received: 28 October 2019 / Accepted: 23 February 2020 / Published online: 7 March 2020
© The Korean Institute of Metals and Materials 2020

Abstract

In the current study, aluminium 6063 alloy (AA6063) was successfully gain refined by twist extrusion (TE) technique. TE is a representative severe plastic deformation process to fabricate ultrafine-grained in bulk materials by repetitive passes. In order to investigate the influence of back pressure, a direct extrusion (DE) channel was embedded after the twist zone and the behavior of AA6063 was investigated and compared with and without this channel. Analyzing microstructural evolutions by scanning electron microscope and Vickers microhardness evaluations showed that, adding the DE channel increased the hardness distribution and a more homogenous structure was obtained. Finite element analysis was utilized to study the distribution of the equivalent plastic strain (PEEQ) numerically. According to the obtained results, with applying the TE process, strain increase was observed all over the sample surface, whereas modeling the DE channel after the twist zone caused a better homogeneity in the PEEQ distribution of the transverse cross-section. The PEEQ distribution during TE process can be correlated to the extent of grain refinement and the uniformity of ultrafine grains. This method seems to be very interesting and very promising for the future industrial application.

Keywords Severe plastic deformation · Twist extrusion · Aluminium 6063 alloy · Back pressure · Finite element analysis

1 Introduction

Severe plastic deformation (SPD) techniques have been the focus of attention during the last decades by virtue of their exceptional abilities in hardening, enhancement of mechanical properties and microstructural development [1–4]. The principal mechanism of grain refinement via SPD includes an increase in dislocation density at the earlier stage of deformation and then the formation of cells and subgrains with low angle grain boundaries during subsequent deformations. More dislocations are generated during further deformations leading to an increase in misorientation between the cells promoting the formation of grains surrounded by high angle grain boundaries [5]. Generally, high shear strains make grain refined materials so that, they insure achieving the structures with micron and in some conditions nano dimensions in microstructure of metals and alloys [6, 7]. The unique characteristic of SPD processes is retaining the size

of the sample till the end of the process, which provides the ability to repeat the process to accumulate higher and more homogeneous strain [8–10].

Processing by twist extrusion (TE) is especially attractive because the procedure can be easily scaled-up to produce relatively large billets and the process present a potential for producing materials which can be used in structural and functional applications [11]. In this process, a billet is pressed through a die with two straight channels separated by a section with helical geometry. For this, straight channels should be long enough [12]. The main deformation during TE occurs precisely at the boundaries between the straight and the twist parts. In addition, a sample can have square, hexagonal, circular and even oval cross-section in TE process [13].

The main distinguishing characteristic of TE process is the vortex flow. If the vortex flow is not closed in the die, the sample after the TE will have a helical shape [14, 15]. In order for the sample to be straight after exiting the twist die, it is necessary that after the helical section of the die there should be a sufficiently long straight section. In addition, a sufficiently large back pressure (BP) must be applied [12]. If the sufficient BP is not applied, the billet cannot obey the die

✉ Mehran Nouri
Nouri@alum.semnan.ac.ir

¹ Faculty of Materials Science and Engineering, Semnan University, Semnan 35131-19111, Iran

geometry especially since the compressive force exerted from the punch cannot provide enough radius force in the whole billet. If the BP is sufficient, the sample will swell and imposes pressure to the die walls leading to a high friction increase which prevents from the formation of metallic dead zones at the die corners [16]. Latypov et al. conducted a research on the BP effects in TE process and found that in addition to the twist strain obtained during the deformation, the imposed BP from the die creates tensile radial strain and compressive axial strain in the sample [17]. This method has many advantages over conventional SPD methods such as using longer samples as compared with high pressure torsion (HPT) process [18, 19], also the ability to extrude the hollow parts and the rectangular cross-sections as compared with equal channel angular extrusion (ECAE) process [20], it can be claimed that TE has higher industrial capabilities.

It should be noted that, mechanical and structural properties of the TE-processed alloys are improved but a high anisotropy occurs in the properties distribution in the cross-section which is not suitable at all [21, 22]. That is why, utilizing a deformation process beside TE is a good solution to this matter [23, 24]. Kim et al. carried out a research in which simple shear extrusion had been done to make the deformation and the strain distribution more homogenous and uniform [25].

Aluminium alloys are used in a variety of structural applications ranging from building and automotive to aerospace industries [26]. Almost two third of aluminium alloys used are 6xxx series, which contain silicon and magnesium in the proportion required to form magnesium silicide, and exhibit good specific strength, toughness, higher corrosion resistance, better weld ability, and above all, it is cheaper as compared to 2xxx and 7xxx series [27–29].

In this paper, by applying enough BP on the whole cross-section of the aluminium 6063 alloy (AA6063), conditions for having the final square geometry became possible. This alloy is commonly used in extrusion process [30, 31]. Since the attractive properties such as high strength and easy formability, AA6063 is a suitable choice for structural applications [32–34]. When AA6063 is subjected to SPD processes, it represents grain refinement resulting in favorable and better mechanical properties [35, 36]. Understanding the plastic strain distribution during the SPD process is essential to optimize the process outcome for specific applications. Researchers have used finite element analysis (FEA) techniques to simulate the deformation behavior and strain distribution during SPD process [37–41].

2 Experimental Work

AA6063 was received in the form of extruded billets with the cross-section of 14.6 mm × 14.6 mm and 50 mm length and the chemical composition as indicated in Table 1.

After their preparation, the samples were full annealed before conducting the tests to make sure that all evolutions would be obtained from TE process. For this purpose, the samples were annealed at 413 °C for 3 h and cooled down in air to ambient temperature. In the next step, the whole surface of the samples was covered with MoS₂ lubricant to minimize the friction, then they were put into the inlet zone of the die and were guided to the twist zone by the steel punch with constant speed of 65 mm/min. Schematic of the TE die used in this study can be observed in Fig. 1. The billet was pushed into the die through a track of 11 mm with the slope angle of $\beta = 30^\circ$ and counter clockwise rotation angle of $\alpha = 90^\circ$ around the extrusion direction and then was sent out of the twist zone. In order to maintain the shape of the billet until the end of the TE process, a direct extrusion (DE) channel was embedded immediately after the twist zone at the bottom of the TE die. At this stage, the cross-section decreased from 14.6 mm × 14.6 mm to 12.6 mm × 12.6 mm. TE process was done using a press machine with the capacity of 100 tons at room temperature.

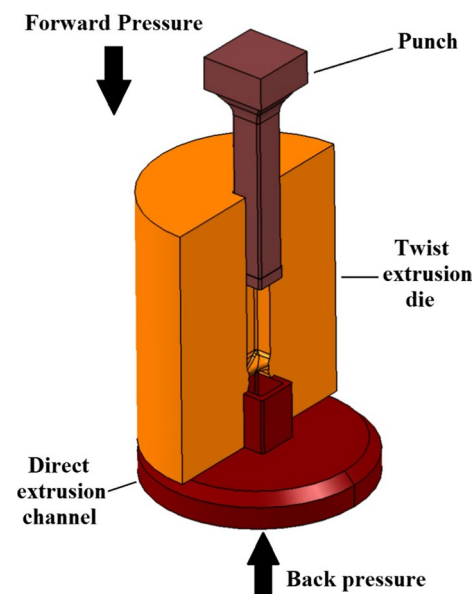


Fig. 1 Schematic of the twist extrusion die and the direct extrusion channel (back pressure)

Table 1 Chemical composition of aluminium 6063 alloy used in this research (wt%)

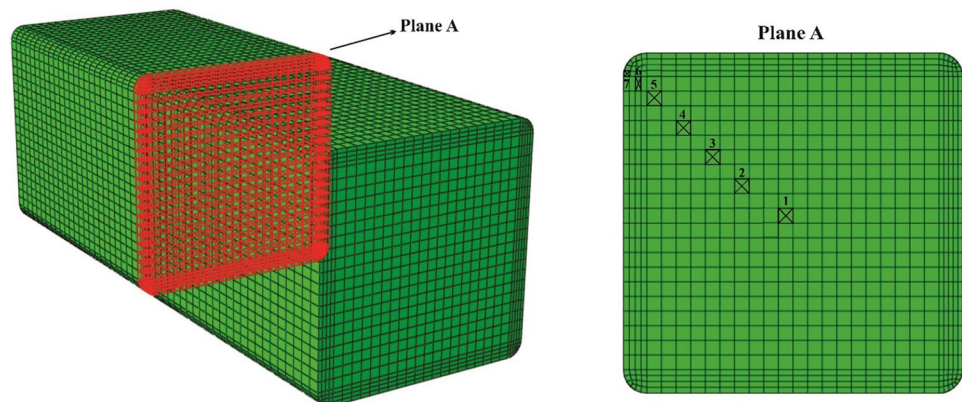
Si	Mg	Fe	Mn	Ti	Cu	Zn	Cr	Al
0.58	0.55	0.20	0.07	0.02	0.01	0.01	0.01	Bal.

To investigate the resultant microstructural evolutions of the TE process, a cross-section with a thickness of 5 mm was chosen from the center of both samples with and without the BP, perpendicular to the extrusion direction and then abrasive and polishing by the Keller's etchant were performed. Metallographic and microstructural observations were well handled utilizing scanning electron microscope (SEM) with the model of ZEISS. Vickers microhardness tests were conducted on the center and four corners of the polished samples, using Buehler digital microhardness tester with the model of MMT7 and load of 50 gr and maintaining time of 25 s.

3 Finite Element Analysis Details

The FEA package ABAQUS explicit was used to simulate the TE process. Due to the complexity of the die geometry its modeling was considered as discrete rigid. Rigid bodies do not need to have material's property leading to an easier and faster analysis. For a better determination of the contact between the sample and the die, a dynamic explicit solver with tangential friction coefficient of 0.01 was used and for vertical friction parameter the type of hard contact was suitable. It should be mentioned that the simulation speed of the TE process was like the laboratory condition. Meshing the die was conducted considering a quad element shape with a size of 1 mm. Before and after the twist zone and because of the geometrical complexity of the twist zone, tri angle element shape with size of 0.04 mm was taken into account for this part. For meshing the billet, C3D8R elements with mesh size of 0.75 mm were applied. Because four corners of the sample had the fillets with the radius of 1 mm hence, finer meshes with size of 0.25 mm were chosen for these zones (Fig. 2). The number of independent elements for the billet and the die were 40,400 and 20,592, respectively.

Fig. 2 Perspective view of the meshed sample before the twist extrusion simulation and selecting elements in middle transverse cross-section (plane A)



4 Finite Element Analysis Results and Discussion

First of all, in order to determine the amount of BP, several conditions of TE were simulated before performing the experimental part. To preserve the primary shape of the billet until the end of the process, BP of 420 MPa should be exerted on the whole cross-section of the sample after exiting the helical section.

After completing the TE process, the final shape of the samples was quite similar to the results of TE simulation. A comparison between simulation and experiment results showed only a slight difference in the appearance of the billets. Figure 3a, b show the images of the billets after the experiment, while Fig. 4a, b show how the strain is distributed at the samples surface from the beginning to the end of the process. Figure 4a, b also show the final shape of the billets in the TE process with and without applying BP.

As it is observed in Fig. 4a, according to the simulation of the TE die without BP, the sample is destroyed and turns into a cylinder with the same length obtained in the experimental work. In this situation, the vortex flow is not closed in the die, that is why the sample has a helical shape in the presented work. But However, TE simulation is modeled along with the DE channel and exerting enough BP which insure the initial geometry of the sample until the end of the process (Fig. 4b).

According to Fig. 2 studying and comparing the changes in equivalent plastic strain (PEEQ) distribution are handled choosing plane A from both samples without the BP (state I) and with the BP (state II). By the movement of the samples through the TE die and when plane A approaches the twist zone, strain distribution is observed in those (Fig. 5a, b). As it is seen from Fig. 5c–e, due to the special mechanism of the TE deformation and high friction force, PEEQ increases specially at the corners. In the following, sample of state II enters the DE channel after crossing the twist zone, at this stage because of the cross-section reduction the sample

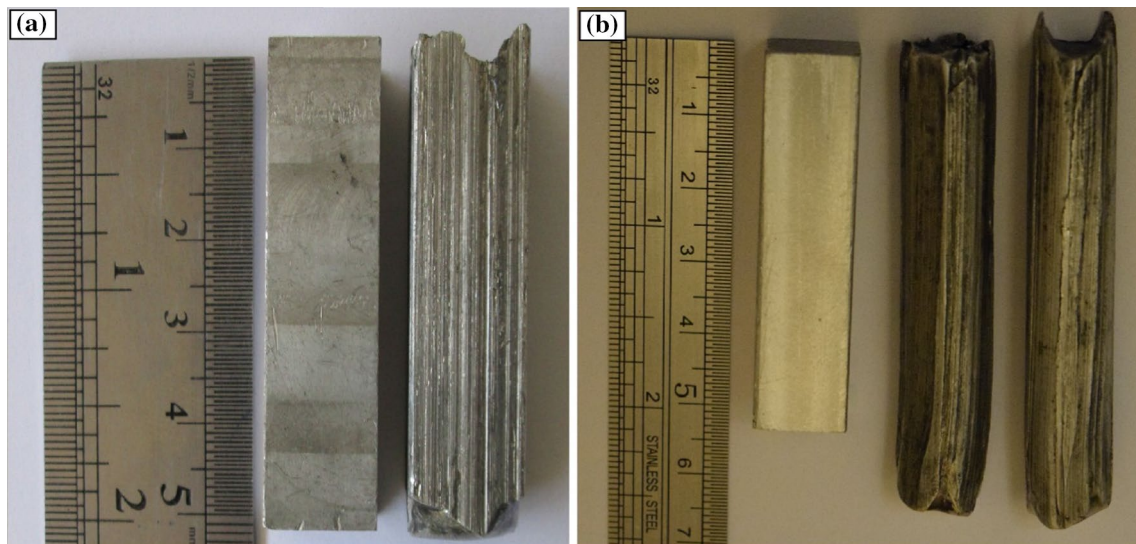


Fig. 3 Annealed samples with; **a** TE-processed sample with the direct extrusion channel and back pressure and **b** TE-processed without the direct extrusion channel and back pressure

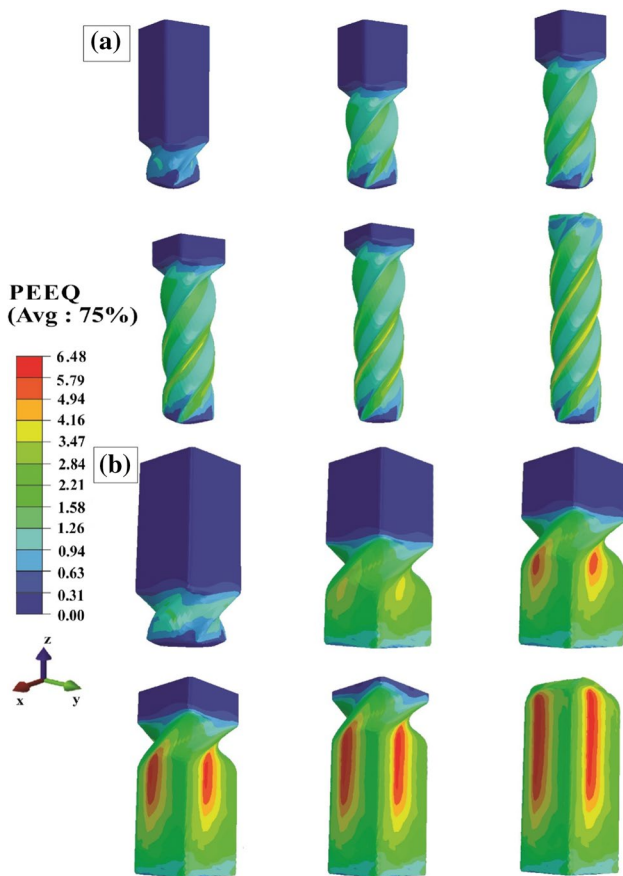


Fig. 4 Equivalent plastic strain distribution (PEEQ) and deformation of the billets; **a** twist extrusion without the direct extrusion channel and back presser and **b** twist extrusion with the direct extrusion channel and enough back presser

undergoes higher work hardening (Fig. 5g). Eventually, upon completion of the TE process PEEQ distribution of the samples can be viewed in Fig. 5h.

In consonance with Fig. 5 during the TE simulation, PEEQ changes increase in both states of I and II. To determine the difference between both states of the TE, an imaginary line is plotted from the maximum element of PEEQ to the central element of plane A and strain distribution is examined on a few elements of that line (Fig. 2).

In the following, the maximum value of PEEQ in all selected elements is compared (Fig. 6). In state I a difference of 94% is observed in the maximum PEEQ of the corner and center elements, whereas the sufficient BP in state II decreases this difference to 55% in those elements. In this study, strain distribution results are in agreement with the study that Beygelzimer et al. did [11] that the maximum strain was at the corner and the minimum was observed at the center being related to inhomogeneous strain distribution of the TE process.

5 Experimental Results and Discussion

In this research before conducting TE process, the microstructure of the plane A was investigated. As it is seen in Fig. 7 the full annealed sample consists of separate coarse grains with average grain size of 314.2 μm .

A recent research [42] reported that in addition to the grain refinement, elongation of grains in the microstructure of a TE-processed pure copper occurred, while the grain arrangement of AA6063 does not show such an elongated structure in state I and coarse and inhomogeneous grains are observed in plane

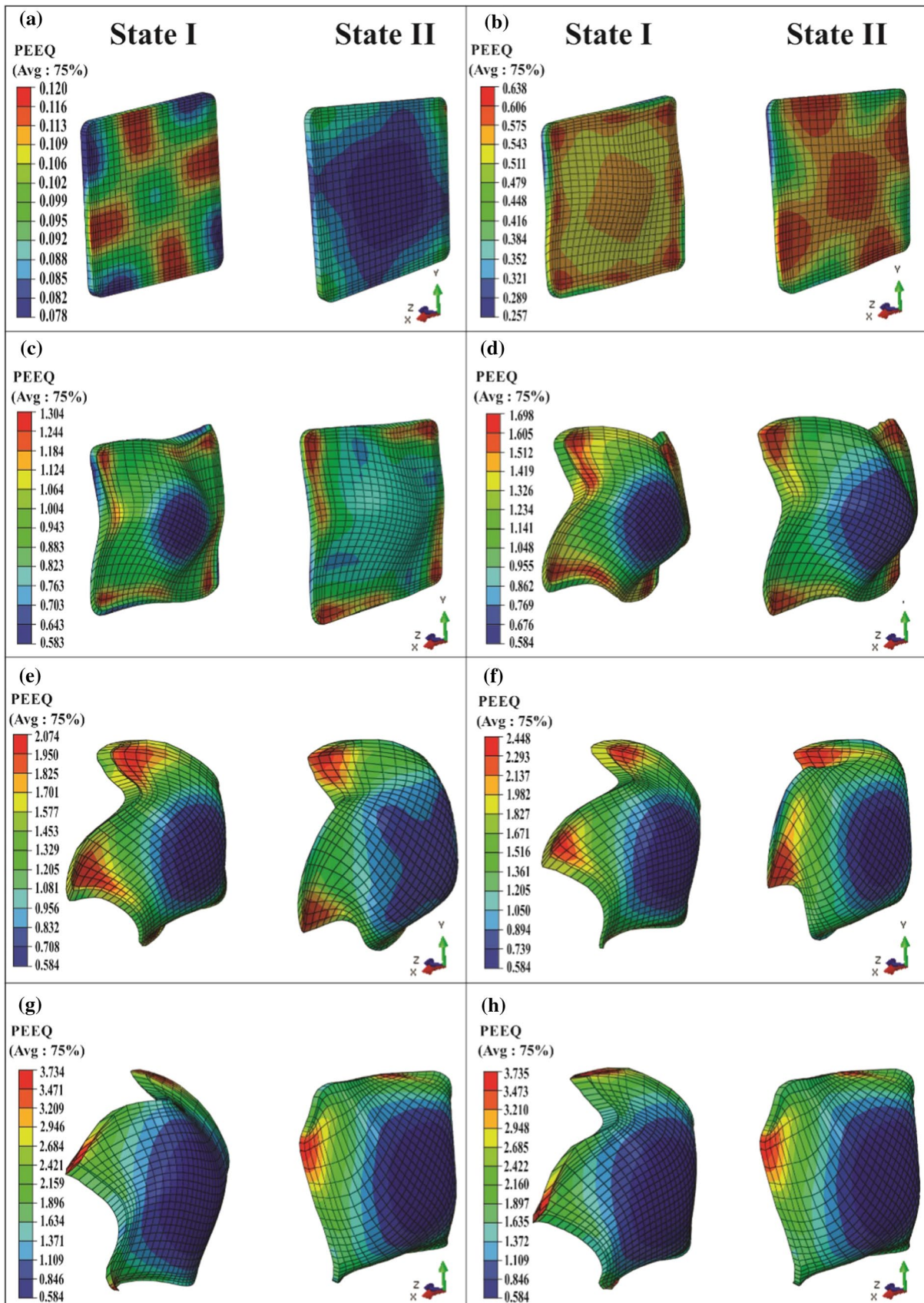


Fig. 5 Comparison of deformation and equivalent plastic strain distribution (PEEQ) in plane A; **a** before the twist zone, **b** at the twist zone entrance, **c–e** in the twist zone, **f** at the moment of exiting from the twist zone, **g** in the DE channel and **h** at the end of the TE process

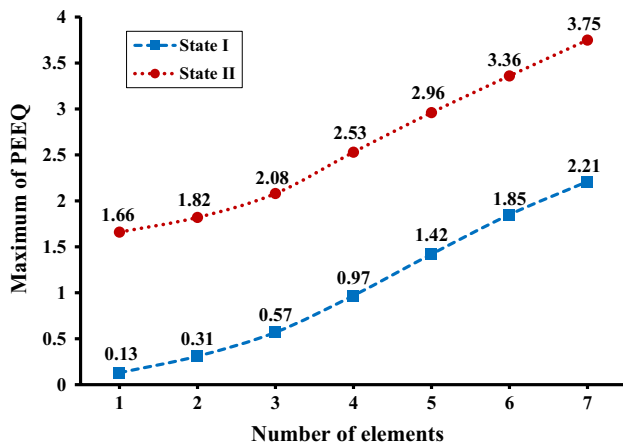


Fig. 6 Maximum values of equivalent plastic strain distribution in selected elements of plane A in states I and II

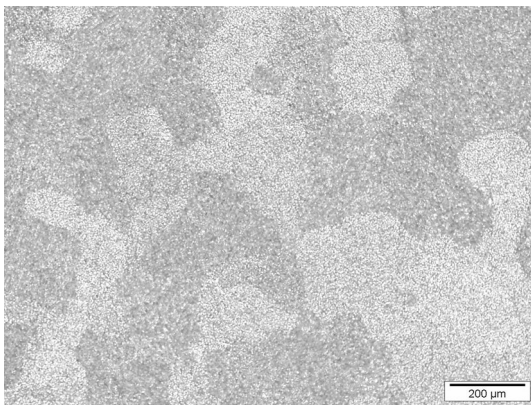


Fig. 7 Initial microstructures of the annealed sample from the cross-section perpendicular to the extrusion

A. In a similar study [43] that Orlov et al. did on commercially pure aluminium, nonexistence of the BP in the first TE pass changed the geometry of the sample and no homogeneity was observed in the microstructure. But about the state II, by dimension reduction of the sample after the twist zone, completely different structure of grain size and shape is obtained.

It is clear from Fig. 8 that in addition to enhanced grain refinement, grains with regular and purposeful orientation are obtained by the direct extrusion. Mousavi [44] applied direct extrusion as a conventional way of deformation after the TE process which made finer grains and more uniform structure in aluminium structure. The grain refining process

of the TE technique is a severe non-uniform deformation process. The elongated grains with an average grain size of 159.6 μm were obtained in the state I, whereas a more homogeneous microstructure with an average grain size of 31.8 μm was observed in the state II.

Vickers microhardness has been distributed homogeneously in all over the cross-section and almost no anisotropy is seen. The average hardness is 34.1 HV. To minimize the error possibility, all the results were reported from the average of five microhardness tests but due to the inhomogeneous deformation in state I, microhardness changes were very dispersed that is why the average hardness was reported from logical results. It has been reported that vickers microhardness distribution along the transverse cross-section of the TE-processed sample is inhomogeneous as well as the grain refinement [45]. In a same study [46], Nouri et al. searched on the TE behavior of the AA6063 and figured out that microhardness changes increase inhomogeneously by the motion of the sample through the twist zone so that microhardness is more in lateral regions as compared with the central regions. To determine the amount of hardness, microhardness tests are carried out in both lateral and central regions. According to Fig. 9 hardness distribution is more inhomogeneous in state I, so that the hardness in lateral and central regions are 42.4 HV and 37.1 HV, respectively. Due to the direct relation between the hardness and dislocations, it can be concluded that less hardness in central regions is because of the low density of dislocations in this region [47]. Besides, microhardness in state II increases to about 69.7 HV and 66.3 HV in lateral and central regions, respectively. Hardness difference in transverse cross-section is due to the higher applied strain in lateral regions in comparison with the central regions [48].

6 Conclusions

Twist extrusion process has been experimentally and numerically carried out on aluminium 6063 alloy with and without back pressure at room temperature. The results are summarized as follows:

1. Successful completion of the twist extrusion process required an appropriate back pressure applied on the whole cross-section of the billet after exiting the helical section. The back pressure should be sufficiently exerted to allow the sample to rotate in the helical zone and

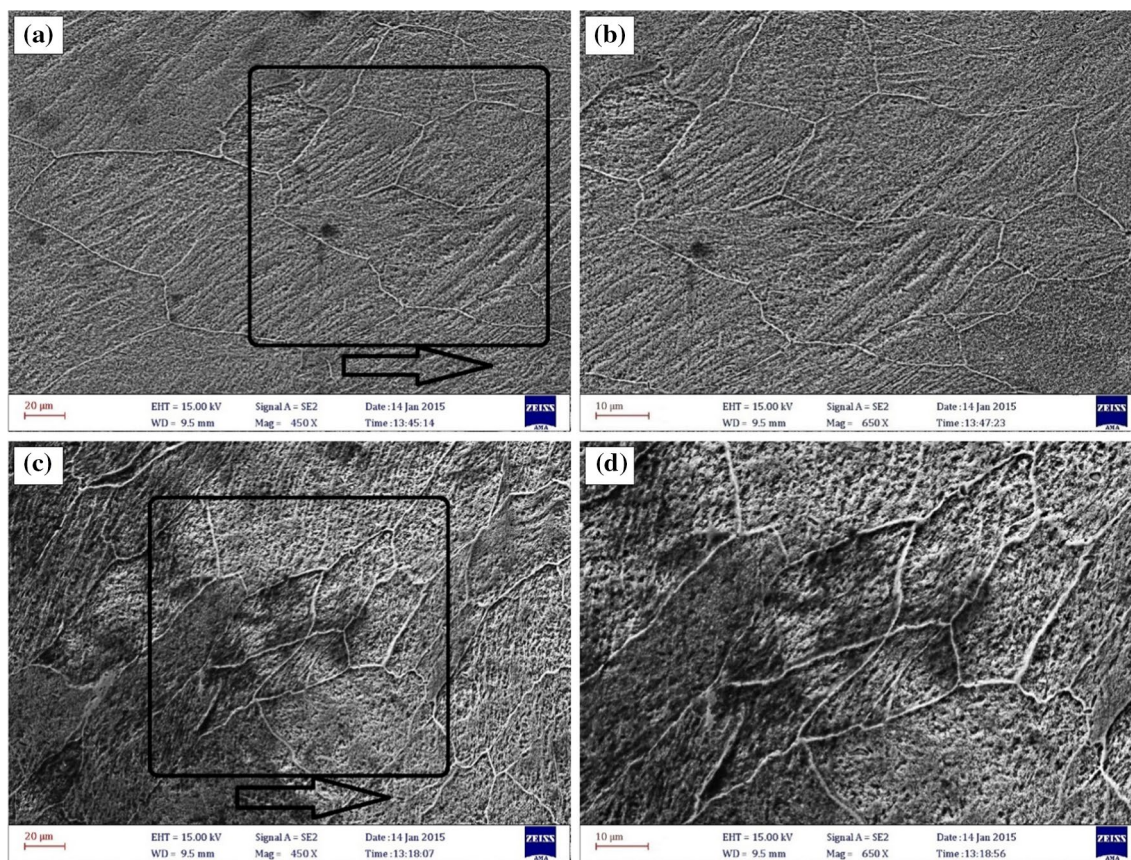


Fig. 8 SEM images of the microstructure after the twist extrusion process; **a, b** twist extrusion without back pressure (state I), **c, d** twist extrusion with back pressure (state II)

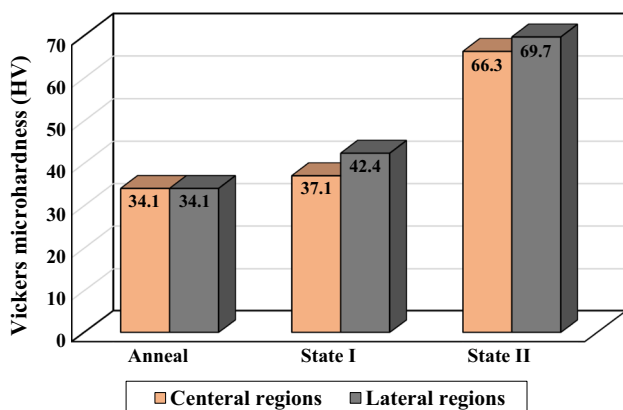


Fig. 9 Vickers microhardness results in lateral and central regions of plane A in annealed sample and states I and II

maintain the sample shape until the end of the process. Considering all the conditions in the simulation of the twist extrusion technique and using a press machine (capacity of 100 tons), back pressure of 420 MPa equivalent to the billet in the opposite direction of extrusion was calculated and applied.

2. Finite element analysis of twist extrusion process predicted a large strain value for state II (twist extrusion with suitable back pressure) along with different directions from a specific section (plane A) as compared to the state I (twist extrusion without back pressure) due to the high shear strain condition in the twist extrusion as well as the friction and interaction effects.
3. The experimental results from the twist extrusion were in reasonably good agreement with the finite element analysis results. Grain refinement was more visible in the lateral regions of billet where the strain distribution was greater than in the central regions.
4. The twist extrusion technique could effectively refine the grains and improve the microstructure of the aluminium 6063 alloy. After applying enough back pressure, the grain size was reduced from an initial average grain size of 314.2 μm to the final average grain size of 31.8 μm .
5. Vickers microhardness of the aluminium 6063 alloy was increased dramatically by applying back pressure after twist section as compared to the initial condition (twist extrusion without back pressure). Moreover, a quite uniform microhardness distribution was observed along the transverse cross-section of state II.

Compliance with Ethical Standards

Conflict of interest The authors declare that they have no conflict of interest.

References

- R.Z. Valiev, Developing SPD methods for processing bulk nanostructured materials with enhanced properties. *Met. Mater. Int.* **7**(5), 413–420 (2001)
- M.S. Kim, S.C. Kwon, S.T. Kim, S. Lee, H.T. Jeong, S.H. Choi, Effect of forging type on the deformation heterogeneities in multi-axial diagonal forged AA1100. *Met. Mater. Int.* **25**(3), 779–793 (2019)
- Y. Qi, R. Lapovok, Y. Estrin, Microstructure and electrical conductivity of aluminium/steel bimetallic rods processed by severe plastic deformation. *J. Mater. Sci.* **51**(14), 6860–6875 (2016)
- J.A. Munoz, O.F. Higuera, J.A. Benito, D. Bradai, T. Khelfa, R.E. Bolmaro, A.M. Jorge Jr., J.M. Cabrera, Analysis of the micro and substructural evolution during severe plastic deformation of ARMCO iron and consequences in mechanical properties. *Mater. Sci. Eng. A* **740–741**, 108–120 (2019)
- M. Sarkari-Khorrami, N. Saito, Y. Miyashita, M. Kondo, Texture variations and mechanical properties of aluminum during severe plastic deformation and friction stir processing with SiC nanoparticles. *Mater. Sci. Eng. A* **744**, 349–364 (2019)
- I. Balasundar, T. Raghu, On the die design for repetitive upsetting—extrusion (RUE) process. *Int. J. Mater. Form.* **6**, 289–301 (2013)
- J.M. Molina-Aldareguia, M.T. Perez-Prado, R.Z. Valiev, I.P. Semenova, I. Sabirov, High strength ultra-fine grained titanium produced via a novel SPD processing route. *Int. J. Mater. Form.* **3**, 407–410 (2010)
- R.B. Figueiredo, G.C.V. De Faria, P.R. Cetlin, T.G. Langdon, Three-dimensional analysis of plastic flow during high-pressure torsion. *J. Mater. Sci.* **48**(13), 4524–4532 (2014)
- B.P. Ho, H.Y. Um, J.G. Kim, H.Y. Jeong, S. Lee, H.S. Kim, Large deformation behavior of twin-induced plasticity steels under high-pressure torsion. *Met. Mater. Int.* **22**(6), 1003–1008 (2016)
- J. Vratna, M. Janecek, J. Cizek, D.J. Lee, E.Y. Yoon, H.S. Kim, Mechanical properties and microstructure evolution in ultrafine-grained AZ31 alloy processed by severe plastic deformation. *J. Mater. Sci.* **48**(13), 4705–4712 (2013)
- Y. Beygelzimer, A. Reshetov, S. Synkov, O. Prokofeva, R. Kulagin, Kinematics of metal flow during twist extrusion investigated with a new experimental method. *J. Mater. Process. Technol.* **209**, 3650–3656 (2009)
- Y. Beygelzimer, R. Kulagin, Y. Estrin, L.S. Toth, H.S. Kim, M.I. Latypov, Twist extrusion as a potent tool for obtaining advanced engineering materials: a review. *Adv. Eng. Mater.* **19**(8), 1–24 (2017)
- Y. Beygelzimer, R. Kulagin, M.I. Latypov, V. Varyukhin, H.S. Kim, Off-axis twist extrusion for uniform processing of round bars. *Met. Mater. Int.* **21**(4), 734–740 (2015)
- Y. Beygelzimer, V. Varyukhin, S. Synkov, Shear, vortices, and mixing during twist extrusion. *Int. J. Mater. Form.* **1**, 443–446 (2008)
- R. Kulagin, M.I. Latypov, H.S. Kim, V. Varyukhin, Y. Beygelzimer, Cross flow during twist extrusion: theory, experiment, and application. *Metall. Mater. Trans. A* **44a**, 3211–3220 (2013)
- A. Hasani, R. Lapovok, L.S. Tóth, A. Molinari, Deformation field variations in equal channel angular extrusion due to back pressure. *Scr. Mater.* **58**, 771–774 (2008)
- M.I. Latypov, I.V. Alexandrov, Y.E. Beygelzimer, S. Lee, H.S. Kim, Finite element analysis of plastic deformation in twist extrusion. *Comput. Mater. Sci.* **60**, 194–200 (2012)
- R. Kocich, A. Machackova, L. Kuncicka, Twist channel multi-angular pressing (TCMAP) as a new SPD process: numerical and experimental study. *Mater. Sci. Eng. A* **612**, 445–455 (2014)
- Y. Beygelzimer, D. Prilepo, R. Kulagin, V. Grishaev, O. Abramova, V. Varyukhin, M. Kulakov, Planar twist extrusion versus twist extrusion. *J. Mater. Process. Technol.* **211**, 522–529 (2011)
- S.A.A.A. Mousavi, A.R. Shahab, M. Mastoori, Computational study of Ti–6Al–4V flow behaviors during the twist extrusion process. *Mater. Des.* **29**, 1316–1329 (2008)
- F. Javadzadeh-Kalahroudi, A.R. Eivani, H.R. Jafarian, A. Amouri, R. Gholizadeh, Inhomogeneity in strain, microstructure and mechanical properties of AA1050 alloy during twist extrusion. *Mater. Sci. Eng. A* **667**, 349–357 (2016)
- S.V. Noor, A.R. Eivani, H.R. Jafarian, M. Mirzaei, Inhomogeneity in microstructure and mechanical properties during twist extrusion. *Mater. Sci. Eng. A* **652**, 186–191 (2016)
- Y. Yuan, A. Ma, X. Gou, J. Jiang, F. Lu, D. Song, Y. Zhu, Superior mechanical properties of ZK60 mg alloy processed by equal channel angular pressing and rolling. *Mater. Sci. Eng. A* **630**, 45–50 (2015)
- M.I.A.E. Aal, H.Y. Um, E.Y. Yoon, H.S. Kim, Microstructure evolution and mechanical properties of pure aluminum deformed by equal channel angular pressing and direct extrusion in one step through an integrated die. *Mater. Sci. Eng. A* **625**, 252–263 (2015)
- J.G. Kim, M. Latypov, N. Pardis, Y.E. Beygelzimer, H.S. Kim, Finite element analysis of the plastic deformation in tandem process of simple shear extrusion and twist extrusion. *Mater. Des.* **83**, 858–865 (2015)
- J.A. Munoz, M. Avalos, R.E. Bolmaro, Heterogeneity of strain path, texture and microstructure evolution of AA6063-T6 processed by equal channel angular sheet extrusion (ECASE). *J. Alloys Compd.* **768**, 349–357 (2018)
- S.K. Panigrahi, R. Jayaganthan, V. Pancholi, Effect of plastic deformation conditions on microstructural characteristics and mechanical properties of 6063 Al alloy. *Mater. Des.* **30**, 1894–1901 (2009)
- S.S. Lokesh-Vendra, S. Goel, N. Kumar, R. Jayaganthan, A study on fracture toughness and strain rate sensitivity of severely deformed Al 6063 alloys processed by multiaxial forging and rolling at cryogenic temperature. *Mater. Sci. Eng. A* **686**, 82–92 (2017)
- G. Faraji, S. Roostae, A.S. Nosrati, J.Y. Kang, H.S. Kim, Microstructure and mechanical properties of ultra-fine-grained Al–Mg–Si tubes produced by parallel tubular channel angular pressing process. *Metall. Mater. Trans. A* **46**(4), 1805–1813 (2015)
- S. Karabay, M. Zeren, M. Yilmaz, Investigation extrusion ratio effect on mechanical behaviour of extruded alloy AA-6063. *J. Mater. Process. Technol.* **135**, 101–108 (2003)
- Y. Wu, H. Liao, Corrosion Behavior of extruded near eutectic Al–Si–Mg and 6063 alloys. *J. Mater. Sci. Technol.* **29**, 380–386 (2013)
- I. Sabirov, M.T. Perez-Prado, M. Murashkin, J.M. Molina-Aldareguia, E.V. Bobruk, N.F. Yunusova, R.Z. Valiev, Application of equal channel angular pressing with parallel channels for grain refinement in aluminium alloys and its effect on deformation behavior. *Int. J. Mater. Form.* **3**, 411–414 (2010)
- M. Khadyko, D. Morin, T. Borvik, O.S. Hopperstad, Tensile ductility of extruded aluminium alloy AA6063 in different tempers. *Mater. Sci. Eng. A* **744**, 500–511 (2019)

34. L.R. Zeng, Z.M. Song, X.M. Wu, C.H. Li, G.P. Zhang, Room-temperature workability of 6063 alloy for fitting clamps of overhead conductor lines. *Mater. Des.* **65**, 187–192 (2015)
35. M. Das, G. Das, M. Ghosh, M. Wegner, V. Rajnikant, S. Ghosh-chowdhury, T.K. Pal, Microstructures and mechanical properties of HPT processed 6063 Al alloy. *Mater. Sci. Eng. A* **558**, 525–532 (2012)
36. M. Samaee, S. Najafi, A.R. Eivani, H.R. Jafarian, J. Zhou, Simultaneous improvements of the strength and ductility of fine-grained AA6063 alloy with increasing number of ECAP passes. *Mater. Sci. Eng. A* **669**, 350–357 (2016)
37. SCh Yoon, A.V. Nagasekhar, H.S. Kim, Finite element analysis of the bending behavior of a workpiece in equal channel angular pressing. *Met. Mater. Int.* **15**(2), 215–219 (2009)
38. H.H. Lee, W. Kim, KCh Jung, S. Seo, J.K. Lee, H.L. Park, K.T. Park, H.S. Kim, Circumferential twisting during route B equal-channel angular pressing. *J. Mater. Process. Technol.* **259**, 305–311 (2018)
39. U.M. Iqbal, V.S. Senthil-Kumar, S. Gopalakannan, Application of response surface methodology in optimizing the process parameters of twist extrusion process for AA6061-T6 aluminum alloy. *Measurement* **94**, 126–138 (2016)
40. A.V. Nagasekhar, H.S. Kim, Analysis of T-shaped equal channel angular pressing using the finite element method. *Met. Mater. Int.* **14**(5), 565–568 (2008)
41. Yu Ivanisenko, R. Kulagin, V. Fedorov, A. Mazilkin, T. Scherer, B. Baretzky, H. Hahn, High pressure torsion extrusion as a new severe plastic deformation process. *Mater. Sci. Eng. A* **664**, 247–256 (2016)
42. S.A.A.A. Mousavi, S.R. Bahadori, The effects of post annealing on the mechanical properties, microstructure and texture evolutions of pure copper deformed by twist extrusion process. *Mater. Sci. Eng. A* **528**, 1242–1246 (2011)
43. D. Orlov, Y. Beygelzimer, S. Synkov, V. Varyukhin, N. Tsuji, Z. Horita, Plastic flow, structure and mechanical properties in pure Al deformed by twist extrusion. *Mater. Sci. Eng. A* **519**, 105–111 (2009)
44. S.A.A.A. Mousavi, Sh Ranjbar-Bahadori, A.R. Shahab, Numerical and experimental studies of the plastic strains distribution using subsequent direct extrusion after three twist extrusion passes. *Mater. Sci. Eng. A* **527**, 3967–3974 (2010)
45. Sh Ranjbar-Bahadori, S.A.A.A. Mousavi, Examination of an aluminum alloy behavior under different routes of twist extrusion processing. *Mater. Sci. Eng. A* **528**, 6527–6534 (2011)
46. M. Nouri, H. Mohammadian-Semnani, E. Emadoddin, H.S. Kim, Investigation of direct extrusion channel effects on twist extrusion using experimental and finite element analysis. *Measurement* **127**, 115–123 (2018)
47. S.R. Bahadori, K. Dehghani, S.A.A.A. Mousavi, Comparison of microstructure and mechanical properties of pure copper processed by twist extrusion and equal channel angular pressing. *Mater. Lett.* **152**, 48–52 (2015)
48. M.S. Mohebbi, A. Akbarzadeh, Experimental study and FEM analysis of redundant strains in flow forming of tubes. *J. Mater. Process. Technol.* **210**, 389–395 (2010)

Publisher's Note Springer Nature remains neutral with regard to jurisdictional claims in published maps and institutional affiliations.